# On the Network Characterization of Planar Passive Circuits Using the Method of Moments

George V. Eleftheriades, *Member, IEEE*, and Juan R. Mosig, *Senior Member, IEEE*

*Abstract*—**The issue of characterizing multiport planar circuits using the method of moments is addressed. For this purpose two commonly encountered excitation models, the delta-gap voltage, and the impressed-current ones are considered. The two excitation models are thoroughly examined and the conditions are determined under which they become equivalent. Based on this equivalence, it is shown how to correctly use the models for extracting the required network representation of general multiport planar circuits, possibly having transversely multisegmented ports, in an unambiguous way. Supportive numerical and experimental results for the characterization of shielded planar circuits are also provided.**

## I. Introduction

In this paper, we study in detail the problem of characterizing multiport planar microwave circuits with the method of moments (MoM) using two commonly encountered excitation models, the delta-gap voltage and the impressed-current models. This includes the treatment of multiport circuits for which some of the physical ports are transversely multisegmented. The problem under consideration concerns the general passive multiport microwave planar circuit of Fig. 1. Our main interest is for shielded monolithic microwave/millimeter-wave integrated circuits (MMIC's), however, the same considerations apply to open microstrip-circuits and to microstrip-fed printed antennas as well. This kind of planar circuit communicates with the external world through $M$ physical ports attached to an equal number of *intrinsic* microstrip feed-lines as shown in Fig. 1. The MoM should now be invoked for characterizing this general planar circuit as an $M$-port network. Specifically, one seeks for relations among the terminal voltages and currents of the form

$$\begin{bmatrix} Z^t_{11} & Z^t_{12} & \cdots & Z^t_{1M} \\ Z^t_{21} & Z^t_{22} & \cdots & Z^t_{2M} \\ \vdots & \vdots & \vdots & \vdots \\ Z^t_{M1} & Z^t_{M2} & \cdots & Z^t_{MM} \end{bmatrix} \begin{bmatrix} I^t_1 \\ I^t_2 \\ \vdots \\ I^t_M \end{bmatrix} = \begin{bmatrix} V^t_1 \\ V^t_2 \\ \vdots \\ V^t_M \end{bmatrix}$$

or

$$[Z^t][I^t] = [V^t]. \tag{1}$$

Although (1) implies expressing the network characterization through the definition of a terminal impedance matrix, any other multiport characterization (admittance matrix, scattering matrix, etc.) is equally valid. To establish such a network characterization with the MoM, we examine here the use of appropriate excitation models such as the delta-gap voltage and the impressed-current models.

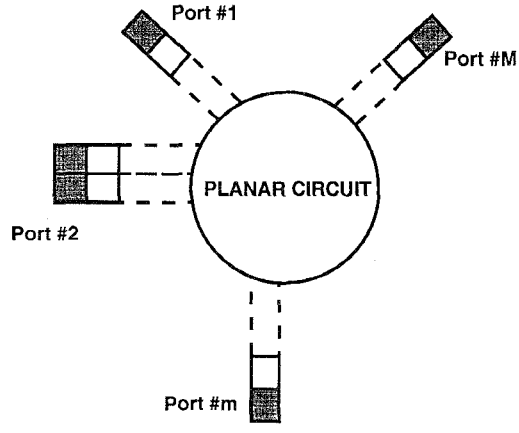


Fig. 1. A general passive $M$-port planar microwave circuit fed by microstrip lines. The intrinsic feed-lines are also considered part of the circuit.

The delta-gap voltage model assumes ideal voltage sources exciting each physical port of the planar circuit. Subsequently, a network representation of the given circuit is directly extracted from the associated moment matrix. Due to its simplicity, the delta-gap voltage model has been adopted by many researchers and a partial listing of the corresponding work is given in [1]–[6]. On the other hand, the impressed-current model assigns known excitation currents at each physical port and the general idea can be found described in [7]–[9]. Subsequently, the corresponding network parameters can be obtained either through the definition of the terminal impedance matrix elements of (1) or from familiar variational expressions derived from the reciprocity theorem.

A widely adopted technique for extracting network parameters from multiport microwave circuits is to extend the physical length of the intrinsic circuit feed-lines (see Fig. 1) so that incident and reflected traveling waves can be identified and then apply ideal transmission line theory. This can be done either by exciting the ports using the delta-gap voltage [6] or the impressed-current [9] models and is easily applicable to ports which are transversely multisegmented. However, this approach requires to include in the analysis sufficiently large transmission-line sections so that a recognizable standing-wave is established on them, thus stressing an already computationally intensive effort [5], [10]. Also, it becomes difficult to extend this method in the case of circuits embedded by multiple coupled transmission line sections [11]. In this paper, our focus is on the characterization of multiport circuits

Manuscript received June 11, 1995; revised November 27, 1995. This work was supported by the European Space Technology Center (ESTEC) Contract 9247/90/NL/US(SC)-Part II.

The authors are with the Laboratoire d' Electromagnetisme et d' Acoustique, Ecole Polytechnique Fédérale de Lausanne, CH-1015 Lausanne, Switzerland.

Publisher Item Identifier S 0018-9480(96)01547-5.

*directly* from the delta-gap voltage or the impressed-current models. In case that there is a need to change the reference planes or even to extract any numerical parasitic effects from these mathematical excitation models, one can resort to numerical de-embedding techniques such as the ones described in [5], [10], [12]. This last possibility renders the use of the direct characterization of multiport circuits, considered in this paper, an attractive alternative to the method of identifying forward and backward traveling waves.

An outline of the present paper is as follows: In Section II, a realistic excitation mechanism involving the transition from a coaxial-line to a microstrip line is considered and related to the two mathematical excitation models under consideration, namely, the delta-gap voltage and the impressed-current models. In Section III, the delta-gap model is described for the network characterization of multiport planar circuits. The impressed-current model and its intimate relation to the delta-gap voltage model are described in the subsequent Section IV, where also the conditions are determined under which the two models become completely equivalent. Section V deals with some aspects of using familiar variational expressions for extracting the network parameters with the MoM and the impressed-current model. The established equivalence between these two excitation models enables to extract network parameters from multiport planar circuits in an unambiguous way. Some further ramifications of this equivalence are discussed in Section VI. Section VII extends the discussion to the more general problem of characterizing multiport circuits for which some of the physical ports are transversely multisegmented. The final Section VIII is devoted to some numerical examples of treating multisegmented ports in shielded planar circuits. The numerical results are also experimentally verified.

## II. Excitation Mechanism and Associated Mathematical Models

In this paper we consider that each microstrip feed-line is attached to the corresponding port through a lateral microstrip to coaxial transition as shown in Fig. 2. This type of feeding configuration is compatible with microstrip shielded and open circuits or with patch antennas fed by microstrip lines. What is important to point out is that the ground-plane is extended up to the tip of the microstrip feed-line and thus there is no space left between the feed-line and the ground-plane. Physically, the excitation is provided by the fields in the coaxial aperture. The scattering parameters of the microwave circuit can then be unambiguously defined based on the incident and reflected TEM waves in the coaxial-lines many wavelengths away from the transition to the microstrip lines. However, the exact solution of the corresponding boundary value problem complicates the analysis and simpler mathematical excitation models, such as the delta-gap voltage model, can still provide excellent computational results [3], [4]. These models can be derived by assuming that at the transition of the coaxial to microstrip line, only the TEM mode is excited. This implies that the pattern of the coaxial aperture fields is known and naturally leads to the magnetic frill model, which can be reduced to the well-known delta-gap voltage excitation model (for a comprehensive review of the process see, for example, [16]). The impressed-current model can be further derived by assuming that instead of known excitation fields (as is the case of the delta-gap voltage model), the terminal currents are known (i.e., impressed), whereas the terminal voltages are unknown and have to be computed. In fact, in this paper, we consider the well-established delta-gap voltage model as the fundamental one [16] and then we try to properly define an equivalent impressed-current model derived from the delta-gap model.

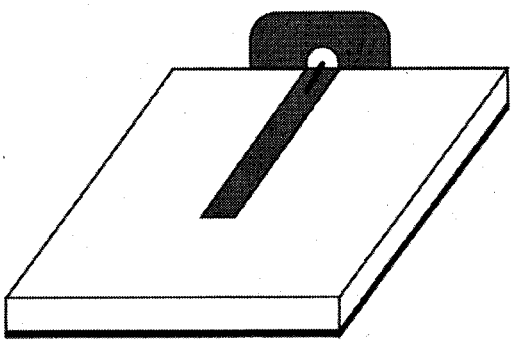

Fig. 2. The physical excitation mechanism for each port.

## III. The Delta-Gap Voltage Excitation Model

Consider the general multiport circuit of Fig. 1. For the moment, it is assumed that each physical port is modeled using a single cell. The case of modeling a physical port with more than one transverse cells is treated in Section VII. The goal of the MoM analysis is to represent the planar circuit by an equivalent network matrix relating, for example, the port voltages and currents as shown in (1). In the delta-gap model, the general port $P_m (m = 1, \cdots, M)$ is assumed to be excited by a voltage source of magnitude $V_m^t$, applied within an infinitesimally small gap of length $\delta \to 0$ and across the extended ground-plane and the tip of the $m$th feed-line, as shown in Fig. 3. Also shown in Fig. 3 is the corresponding expansion of the induced circuit current with some arbitrary kind of subsectional basis-functions in the framework of the MoM. The delta-gap voltage source at each port provides an impressed (or incident) excitation field described by the expression

$$\bar{E}^{\text{inc}} = V_m^t \delta(\bar{r} - \bar{r}_m)\hat{n}_m \tag{2}$$

where $\bar{r}_m$ is the location of the port and $\hat{n}_m$ is the outward normal parallel to the corresponding feed-line. As shown in the same Fig. 3, an induced terminal current $I_m^t$ flows through the voltage source, which spreads into a half-subsectional basis function also located at $\bar{r}_m$. The corresponding electric field integral equation (EFIE) governing the surface current, $\bar{J}_s$, on all conductor surfaces is then given by

$$\int_{S_c} \overline{\overline{G}}_{EJ}(\bar{r}, \bar{r}') \cdot \bar{J}_s(\bar{r}')\, ds' = -\sum_{m=1}^{M} V_m^t \delta(\bar{r} - \bar{r}_m)\hat{n}_m \tag{3}$$

where $\overline{\overline{G}}_{EJ}$ is the pertinent transverse part of the electric field Green's function and $S_c$ denotes all circuit-cells including the feed-line and port ones. The left-hand side of (3) represents the tangential electric field due to all induced currents (customarily

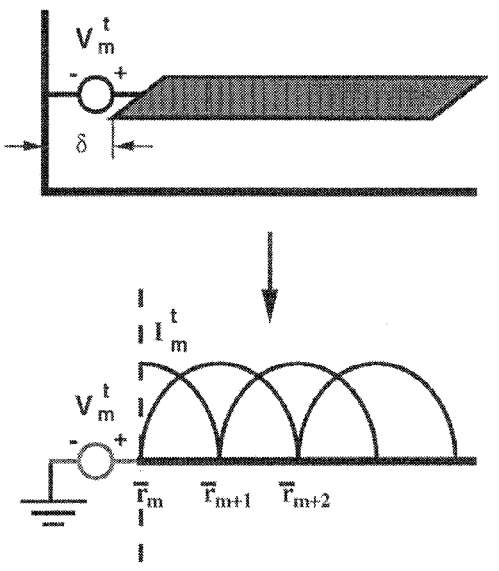


Fig. 3. A delta-gap voltage source exciting the general port #$m$ and the associated MoM description. For the MoM description, the quantities that participate in the excitation process are shaded.

referred to as the scattered field $\bar{E}^{\text{scat}}$) whereas the right-hand side is the impressed tangential electric field defined by (2). Thus (3) expresses the usual condition of vanishing tangential electric field on the conducting circuit surface, $\bar{E}^{\text{inc}} + \bar{E}^{\text{scat}} = 0$. To be more specific about this condition, the observation point $\bar{r}$ of the EFIE (3) runs all-over the entire surface $S_c$, which implies that the same condition *also extends to the location* of the induced half-subsectional currents at $\bar{r}_m$. From a mathematical point of view, this is necessary because otherwise (3) would only admit the trivial solution, $\bar{J}_s = 0$. Physically, the same requirement is compatible with the assumption of using ideal exciting voltage sources, which implies that they have *zero* internal resistance.

Now, within the framework of the MoM, the induced surface current is expanded into a set of subsectional basis functions as shown below

$$\bar{J}_s(\bar{r}') = \sum_{m=1}^{M} I_m^t \bar{f}_m(\bar{r}') + \sum_{n=M+1}^{M+N} I_n^c \bar{f}_n(\bar{r}') \tag{4}$$

where, without loss of generality, it is assumed that the width and base value of each basis function are unity. Also, it is assumed that the basis functions in the range $\{\bar{f}_m, m = 1, \cdots, M\}$ represent half-subsections (induced port currents) whereas the rest $\{\bar{f}_n, n = M+1, \cdots, M+N\}$ are full-subsections. In addition, the index, $t$, stands for terminal (or port) quantities that are associated with half-subsectional basis elements whereas the index, $c$, denotes circuit (including the feed-lines) quantities associated with full-subsectional basis elements. Applying the MoM procedure to (3), using the current expansion of (4) and corresponding weighting functions $\{\bar{w}_n, n = 1, \cdots, M+N\}$ yields (5), as shown at the bottom of the page, where the MoM impedance elements are defined by

$$Z_{mn} = -\int_{S_c}\int_{S_c} \bar{w}_m(\bar{r}) \cdot \bar{\bar{G}}_{EJ}(\bar{r}', \bar{r}) \cdot \bar{f}_n(\bar{r}')\, ds\, ds' \tag{6}$$

and the distinction between port (terminal) and circuit quantities is explicitly designated. In block matrix form (5) can be rewritten as

$$\begin{bmatrix} Z^{tt} & Z^{tc} \\ Z^{ct} & Z^{cc} \end{bmatrix} \begin{bmatrix} I^t \\ I^c \end{bmatrix} = \begin{bmatrix} V^t \\ 0 \end{bmatrix} \tag{7}$$

The delta-gap voltage formulation is very convenient because by inverting the associated moment matrix $[Z]$, terminal relations among the port voltages and currents are directly obtained. Indeed, if the moment matrix is inverted as shown below

$$\begin{bmatrix} Y^{tt} & Y^{tc} \\ Y^{ct} & Y^{cc} \end{bmatrix} = \begin{bmatrix} Z^{tt} & Z^{tc} \\ Z^{ct} & Z^{cc} \end{bmatrix}^{-1}. \tag{8}$$

Then $[Y^{tt}][V^t] = [I^t]$ and, therefore, the sub-matrix $[Y^{tt}]$ is nothing but the required network admittance-matrix $[Y^t]$, characterizing the given $M$-port circuit. Likewise, by a simple manipulation of (7) one can also obtain the relation between the terminal voltages and currents in an impedance matrix form that is given below

$$[Z^t] = [Z^{tt}] - [Z^{tc}][Z^{cc}]^{-1}[Z^{ct}]. \tag{9}$$

In practice, the network representation of the given planar-circuit in terms of terminal voltages and currents is converted in a form that involves experimentally observable quantities. This is usually accomplished by converting the network admittance or impedance matrix to a scattering-parameter matrix.

## IV. The Impressed-Current Model and Its Relation to the Delta-Gap Voltage Model

Once more, consider the $M$-port circuit of Fig. 1, again with the assumption that each physical port is modeled using a single cell. In the impressed-current model, half-subsectional

$$\left[\begin{array}{ccc|ccc} Z_{1,1} & \cdots & Z_{1,M} & Z_{1,M+1} & \cdots & Z_{1,M+N} \\ \vdots & & \vdots & \vdots & & \vdots \\ Z_{M,1} & \cdots & Z_{M,M} & Z_{M,M+1} & \cdots & Z_{M,M+N} \\ \hline Z_{M+1,1} & \cdots & Z_{M+1,M} & Z_{M+1,M+1} & \cdots & Z_{M+1,M+N} \\ \vdots & & \vdots & \vdots & & \vdots \\ Z_{M+N,1} & \cdots & Z_{M+N,M} & Z_{M+N,M+1} & \cdots & Z_{M+N,M+N} \end{array}\right] \left[\begin{array}{c} I_1^t \\ \vdots \\ I_M^t \\ \hline I_{M+1} \\ \vdots \\ I_{M+N} \end{array}\right] = \left[\begin{array}{c} v_1^t \\ \vdots \\ v_M^t \\ \hline 0 \\ \vdots \\ 0 \end{array}\right] \tag{5}$$

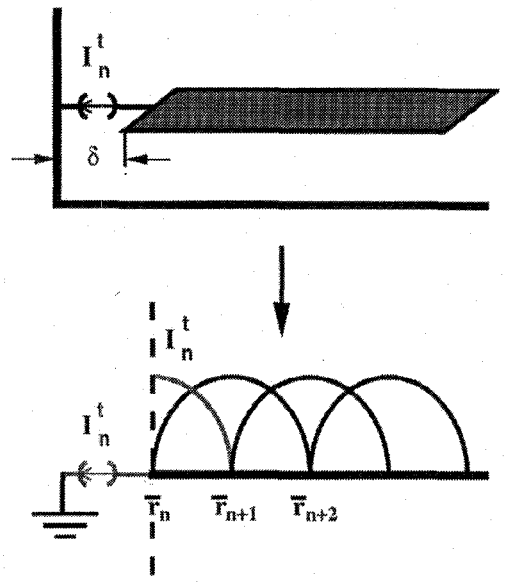


Fig. 4. A current source exciting the general port #$n$ and the associated MoM description. For the MoM description, the quantities that participate in the excitation process are shaded.

currents are assumed impressed at each port and terminal relations of the form described by (1) are sought for characterizing the $M$ physical ports. The exact description of this model is illustrated in Fig. 4. As shown, the $n$th port of the circuit is now assumed to be excited by a current source of magnitude $I_n^t$ existing in the infinitesimal gap between the extended ground-plane and the tip of the microstrip feed-line. The excitation current spreads into an impressed half-subsectional basis function located at the port position $\bar{r}_n$ as shown in the same Fig. 4. The corresponding induced terminal voltage $V_n^t$ is measured across the current source in the infinitesimally small gap region. Note that although the gap length, $\delta$, tends to zero, a nonvanishing finite voltage $V_n^t$ should always be induced in order to establish a finite input-impedance. This means that as the length of the gap-region tends to zero, the induced field across it tends to infinity. The assumptions made so-far, for defining the impressed-current model in Fig. 4, might initially seem rather arbitrary. As will soon become evident, however, they are in fact necessary for establishing equivalence with the delta-gap voltage model.

To proceed further with this model we consider one port excited at a time with the rest of the ports open-circuited. Let the $n$th port be the excited one. Then, the impressed-current is given by $\bar{J}_n^{\text{imp}} = I_n^t \bar{f}_n$ and the $n$th row of the network impedance matrix is determined by definition from the relation

$$Z_{mn}^t = \frac{V_m^t}{I_n^t} \tag{10}$$

with all ports but the $n$th open-cicuited, where $V_m^t$ is the induced terminal voltage at the $m$th port. The corresponding integral-equation for this excitation model, governing the induced circuit current $\bar{J}_s$ is as usually obtained by enforcing a vanishing tangential electric field on the circuit surface $S_c$

$$\int_{S_c} \overline{\overline{G}}_{EJ}(\bar{r},\bar{r}')\cdot\bar{J}_s(\bar{r}')\,ds' = -\int_{S_n} \overline{\overline{G}}_{EJ}(\bar{r},\bar{r}')\cdot\bar{J}_n^{\text{imp}}(\bar{r}')\,ds' \tag{11}$$

where $S_n$ denotes the area of the $n$th port-cell. The left-hand side of (11) is the tangential electric field due to all induced surface currents, whereas the right-hand side is the tangential electric field due to the impressed-current. At this point, it is important to compare the impressed-current integral (11) with the delta-gap voltage integral (3). This time, in order to ensure that (11) has other than the trivial solution, $\bar{J}_s = -\bar{J}^{\text{imp}}$, the observation point $\bar{r}$ should *exclude* the location of the impressed-current $\bar{r}_n$. This requirement is exactly the opposite for the the delta-gap voltage model in which case (3) *has to be enforced* at the location of the voltage source $\bar{r}_m$. From the physical point of view, this admissibility condition for (11) is compatible with the assumption of an ideal current source that provides the impressed-current $\bar{J}^{\text{imp}}$ and has an *infinite* internal resistance. Another noticeable difference between integral equations (11) and (3) is that unlike the case of (3), the induced current $\bar{J}_s$ in (11) only contains full-subsectional basis elements since the half-subsectional ones are assumed to be impressed. Following the discussion of these fine details, we can now proceed with the MoM and expand the induced current into a set of full-subsectional basis functions, i.e.,

$$\bar{J}_s(\bar{r}') = \sum_{q=M+1}^{M+N} I_q^c \bar{f}_q(\bar{r}'). \tag{12}$$

For the sake of clarity and coherence, (12) makes use of the same numbering and symbol conventions as its delta-gap voltage model counterpart of (3). Another important point to mention is that in order to make a meaningful comparison between the two excitation models under consideration, the same expansion basis functions are used for both the delta-gap voltage and the impressed-current models. This automatically implies that in the case of the impressed-current model, the half-subsectional basis elements used for representing the impressed currents belong to the same family as the basis elements used for expanding the induced currents. Applying the MoM now to (11), utilizing the current representation of (12) and the weighting functions $\{\bar{w}_n, n = M+1, \cdots, M+N\}$ yields in matrix form

$$[Z_{pq}^{cc}][I_q^c] = -I_n^t[Z_{pn}^{ct}], \quad (q,p) \in \{M+1,\cdots,M+N\} \tag{13}$$

where the same definition for the MoM elements given in (6) also applies.

From this point on, one way to proceed with the determination of the required network characterization would be to utilize familiar variational expressions derived from reciprocity considerations. Such a possibility will be examined in the next section. However, the most intuitively simple way for determining the required terminal network impedance elements is to resort to the impedance-matrix definition of (10)

$$Z_{mn}^t = \frac{V_m^t}{I_n^t} = -\frac{\int_{S_m} \bar{E}_{\text{total}}\cdot\overline{dl}}{I_n^t}. \tag{14}$$

The field denoted as $\bar{E}_{\text{total}}$ in (14) is the total tangential field generated by both the impressed-current $\bar{J}_n^{\text{imp}}$ and the induced circuit currents $\bar{J}_s$. This field, which is explicitly given in (15)

for clarity

$$\bar{E}_{\text{total}}(\bar{r}) = \int_{S_c} \bar{\bar{G}}_{EJ}(\bar{r}, \bar{r}') \cdot \left(\bar{J}_n^{\text{imp}}(\bar{r}') + \bar{J}_s(\bar{r}')\right) ds' \quad (15)$$

has been enforced by the MoM to vanish on the circuit surface except at the location of the impressed-current and at the corresponding open-circuited current sources across which the induced voltages are measured. To continue the discussion, one should notice that in order to derive (13), we have required that only the moments of the total tangential electric field (15) with the circuit weighting functions $\{\bar{w}_n, n = M+1, \cdots, M+N\}$ do vanish. In the case of the delta-gap voltage model, however, *the complete set* of the weighting functions has been used to enforce the condition of vanishing electric field on the surface of the circuit. With this observation as a guideline, we now proceed to use the rest of the weighting functions associated with the location of the ports $\{\bar{w}_n, n = 1, \cdots, M\}$, in conjunction with (14), in order to retrieve the required network impedance elements. Under these considerations, the inner products between the total electric field $\bar{E}_{\text{total}}$ of (15) and the port weighting functions should vanish everywhere except at the location of the impressed and open-circuited current sources, $\bar{r}_n$, where the induced voltages $V_m^t$ are sampled out. Therefore, one can immediately write the following expression for the induced terminal voltages

$$\begin{aligned} V_m^t &= \langle \bar{w}_m, \bar{E}_{\text{total}} \rangle \\ &= Z_{mn} I_n + Z_{m,M+1} I_{M+1} \\ &\quad + \cdots + Z_{m,M+N} I_{M+N}, \quad m = 1, \cdots, M \\ &= [Z^{tt}] I_n^t + [Z^{tc}][I^c]. \end{aligned} \quad (16)$$

Using these voltages in the defining equation (14) and eliminating the induced circuit currents by virtue of (13), one immediately recovers the network impedance-matrix representation (9) found before with the delta-gap voltage model. Therefore, this treatment of the impressed-current model provides identical results with the delta-gap voltage excitation model. It is reassuring to also observe that the delta-gap voltage model (7) is formally identical to the impressed-current one of (13) and (16) but with the interpretation of the terminal voltages and currents different. For the delta-gap voltage model, the terminal voltages are impressed and the terminal currents are induced, whereas for the impressed-current model the terminal currents are impressed and the terminal voltages are induced.

## V. Network Characterization Using Variational Expressions with the Impressed-Current Model

One problem that the formulation based on the impressed-current model faces is that (14) requires a *direct* access to the electric field in order to define the network impedance elements. Since the MoM does not explicitly provide such an access, it becomes attractive, instead of using (14), to resort to definitions derived from familiar variational expressions for determining the network impedance elements [16]. Such a defining equation is given below

$$Z_{mn}^t = -\frac{\int \bar{E}\left(\bar{J}_n^{\text{imp}}\right) \cdot \bar{J}_m^t \, ds}{I_m^t I_n^t}. \quad (17)$$

However, this option can induce confusion and care should be exercised in its correct interpretation and its application. The conceptual difficulties in applying (17) with the impressed-current model and the MoM mainly arise from the interpretation of the electric field due to the impressed-current $\bar{E}(\bar{J}_n^{\text{imp}})$. If this is the total field (as it should be), then it vanishes on all conducting surfaces and therefore the impressed currents should be physically separated from them, leaving little hope of a direct comparison between the impressed-current and delta-gap voltage models. Such a separation of the impressed-current region from the conducting parts has in fact been found necessary in the work of [9], presumably due to similar considerations. On the other hand, if the impressed currents are not separated from the planar conductors and the electric field is interpreted as originating only from the induced currents $\bar{J}_s$ then the diagonal impedance elements lose their "self-impedance" component (i.e., the interaction of $\bar{J}_m^t$ to itself is lost) and once more the impressed-current and delta-gap voltage models become incompatible.

The correct interpretation of (17) within the MoM and the impressed-current model becomes apparent from the analysis presented in Section IV. In this context and in analogy to (16), equation (17) can be thought of *as being the enforcement* of the condition for a vanishing total electric field, $\bar{E}_{\text{total}}$, everywhere on the support of the port-cells *except* at the locations of the impressed-current sources $\bar{r}_n$. In this case, the role of the port weighting functions in the MoM $\{\bar{w}_m, \ m = 1, \cdots, M\}$ is undertaken by the impressed currents $\{\bar{J}_m^{\text{imp}}, \ m = 1, \cdots, M\}$. In the special case of using Galerkin's technique, i.e. $\{\bar{w}_p = \bar{f}_p, \ p = 1, \cdots, M+N\}$, the impressed-current model of Section IV becomes compatible with the variational expression (17) and consequently so does the delta-gap voltage model of Section III. Furthermore, with Galerkin's method we can use the condition $\{\langle \bar{w}_p, \bar{E}_{\text{total}} \rangle = 0, p = M+1, \cdots, M+p\}$ imposed by the MoM to replace the impressed-current in (17) with the total current $\bar{J}_s + \bar{J}_m^{\text{imp}}$ and extend the support of the integration over the entire circuit surface. This in fact leads to the precise definition of the impedance variational expression which implicates the *entire* surface of the circuit [17]. On the other hand, in the general case of arbitrary weights, the use of (17) corresponds to applying the MoM with a delta-gap model and a mixed type of weighting functions, i.e., $\{\bar{w}_p = \bar{f}_p$ only for $p = 1, \cdots, M\}$. In all cases, care should be exercised so that the total spectrum of weighting functions forms a basis for the range of the EFIE operator [13].

The paractical conclusion of the above arguments is that when using variational expression (17), it is not neccessary to separate the impressed current region from the conducting surfaces. This statement is true despite the fact that $\bar{E}(\bar{J}_n^{\text{imp}})$ in (17) stands for the total electric field.

## VI. Discussion

Up to this point, we have seen how to properly interpret the delta-gap voltage and impressed-current excitation models so that they become equivalent. It should be mentioned that these two models *are not strictly dual* to each other. This is because the dual of the delta-gap voltage model is obtained by interchanging the lumped voltage source in Fig. 3 with

a lumped current source. However, when this is done, the impressed-current model of Fig. 4 is not exactly recovered since the impressed current is *distributed* and extends to the support of the terminal half-subsectional basis function. Nevertheless, with the careful consideration of the impressed-current model described in Sections IV and V, we have been able to establish its one-to-one correspondence to an equivalent delta-gap voltage model. With this equivalence as a guide, we can go one step further and ask the question whether it is legitimate to use an *arbitrary* current distribution as the impressed-current source. In the framework of the present analysis and having in mind the results of [13] on the choice of the expansion functions, it appears that the answer to this question is positive, provided that the impressed currents belong to the span of the basis-functions chosen to expand the domain of the integral operator. Only then, the impressed-current formulation remains consistent with an equivalent *legitimate* delta-gap voltage model.

Another point that in retrospect emerges as worth mentioning is that the delta-gap $\delta$-space depicted in Figs. 3 and 4 can be viewed as merely an artifice introduced for "measuring" impressed or induced port voltages. In view of (16), one can instead consider the *weighting procedure* with the port-cell weights as the fundamental mathematical process of defining terminal voltages and completely avoid the implication of delta-gaps associated with the port cells.

## VII. Treating Multisegmented Physical Ports

In the previous sections, we have assumed that in the framework of the MoM each physical port is represented by a single cell. In many occasions, however, it is desirable to implicate more than one transverse cells, for example, to accurately model the transverse behavior of the current or to comply with the global grid-resolution used for the rest of the circuit. To this end, first consider *a one* physical port circuit having its input port segmented into $M$ transverse cells as Fig. 5 shows. To treat this situation with the impressed-current model, it would seem appealing to assign to each of the $M$ transverse port-cells impressed currents of the type described in Fig. 4 and then utilize (17) to evaluate the input-impedance of the physical port. Such an approach will very quickly reveal that the impressed currents at each of the constituent port-cells cannot be chosen arbitrarily. The reason, of course, being that since the $M$ cells belong to the same physical port, the induced voltages at each cell should be identical. In other words, the port-cells are physically connected in parallel and this constraint has to be taken into consideration. Another interpretation for the same phenomenon would be that the impressed-currents at each of the $M$ cells should be preselected in such a way so that the true transverse behavior of the feed-line longitudinal current is successfully approximated (e.g., Maxwellian distribution in the case of an isolated line).

The simplest way to resolve the multisegmented port situation of Fig. 5 is, perhaps, to resort to the delta-gap voltage model. For this purpose, the physical port should be assumed excited by a distributed delta-gap voltage source of magnitude $V_0$ which induces terminal (port) half-subsectional currents $I_m^t$, as shown in Fig. 6. At this point, the corresponding induced

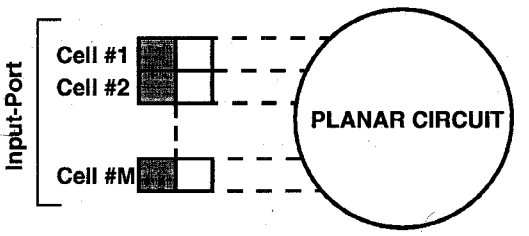


Fig. 5. A one-port circuit with the input port multisegmented with $M$ transverse cells.

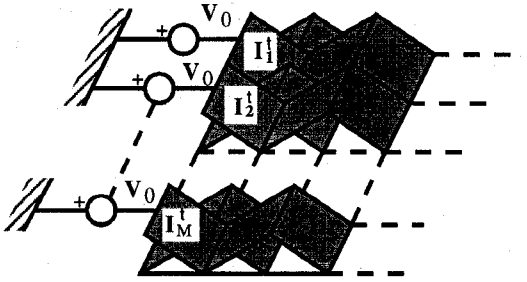


Fig. 6. A multisegmented port excited by a distributed delta-gap generator.

port current is obtained by summing-up all the partial currents $I_m^t$. Therefore, the associated input impedance is determined by

$$Z_{\text{in}} = \frac{V_0}{\sum_{m=1}^{M} I_m^t} \tag{19}$$

which implicitly enforces the condition that the $M$ port-cells are physically connected in parallel. For determining the required currents $I_m^t$ it is assumed that the circuit is modeled using $M$ half-subsections for the induced partial currents and $N$ full-subsections for the rest of the induced currents. Under these assumptions, the MoM equations (5) and (6) are still valid but with the provision that: $\{V_1 = V_2 = \cdots V_M = V_0\}$. The corresponding terminal relationship between the applied voltages and induced port currents is therefore given by

$$[Y^t][V_0] = [I^t]. \tag{20}$$

Within the framework of the MoM, the required input impedance as determined from (19) and (20) is then given by

$$Z_{\text{in}} = \frac{1}{\sum_{p=1}^{N}\sum_{q=1}^{N} Y_{pq}^t} = \frac{V_0^2}{[V_0]^T[Y^t][V_0]}. \tag{21}$$

In conclusion, to characterize a multisegmented physical port with the delta-gap voltage model, each segment should be treated as a separate mathematical port. Eventually these mathematical ports should be combined in parallel in order to obtain the required physical port input-impedance.

Having established the equivalence between the delta-gap voltage and impressed-current models as described in Sections III and IV, we can safely claim that the same procedure for characterizing multisegmented ports can be followed when originating from the impressed-current model. However, such a treatment of multisegmented ports is justified provided that every physical port is electrically narrow so that no transverse currents flow across them. Only then, a unique induced voltage can be defined for each physical port.

The extension of our discussion to the general case of multiport (physical) circuits in which one or more physical ports are transversely multisegmented is quite straightforward. To achieve this, each cell belonging to a physical port should be treated as an independent mathematical excitation port. The resulting augmented multiport circuit should then be characterized using the MoM under either the delta-gap voltage or the impressed-current excitation models. This process determines a corresponding augmented terminal admittance matrix $[Y^t_{\text{aug}}]$ which is uniquely defined, irrespective of the type of excitation model used. Subsequently, the resulting augmented admittance matrix $[Y^t_{\text{aug}}]$ should be reduced to the required network admittance matrix $[Y^t]$ by combining in parallel mathematical ports belonging to the same physical port with the aid of standard circuit theory.

## VIII. Numerical Examples

A simple verification test for the process of handling multisegmented ports, described in the previous Section VII, consists of analyzing a given planar circuit under different grid resolutions and comparing the corresponding results. As an example, consider the shielded microstrip single-stub filter of Fig. 7 [14]. This benchmark circuit is analyzed using the mixed potential integral equation (MPIE) technique in conjunction with Galerkin's procedure and triangular rooftop basis functions [7], [8], [14], [15]. The stub is analyzed under two different uniform grid resolutions. In the first one, a 20 $\times$ 20 grid is employed to discretize the cross section of the shielding rectangular box and this corresponds to implicating only a single cell for modeling the transverse current on the microstrip lines. On the other hand, the second grid resolution corresponds to a doubly-fine 40 $\times$ 40 uniform mesh. This time, two cells are used to model the transverse behavior of the microstrip line currents. According to Section VII, in order to analyze the given circuit under the doubly fine resolution an augmented admittance matrix $[Y^t_{\text{aug}}]$ should first be computed for which each port-cell is treated as an independent mathematical port. A schematic for the associated augmented circuit is shown in Fig. 8. As shown in Fig. 8, the input physical port $(A)$ consists of two transverse cells, 1) and 3), whereas the output port $(B)$ is segmented with cells 2) and 4). The associated augmented admittance matrix is a 4 $\times$ 4 one, corresponding to mathematical ports 1)–4). According to Section VII, in order to obtain the required network 2 $\times$ 2 admittance matrix $[Y^t]$ characterizing physical ports $(A)$ and $(B)$, mathematical ports belonging to the same physical port should be combined in parallel. This means that $[Y^t]$ is determined by

$$\begin{aligned} Y^t_{AA} &= Y^t_{\text{aug},11} + Y^t_{\text{aug},31} + Y^t_{\text{aug},13} + Y^t_{\text{aug},33} \\ Y^t_{AB} &= Y^t_{BA} = Y^t_{\text{aug},12} + Y^t_{\text{aug},14} + Y^t_{\text{aug},32} + Y^t_{\text{aug},34} \\ Y^t_{BB} &= Y^t_{\text{aug},22} + Y^t_{\text{aug},24} + Y^t_{\text{aug},42} + Y^t_{\text{aug},44}. \end{aligned} \tag{22}$$

The computed scattering parameters for the circuit of Fig. 7 as a function of the frequency under the two grid resolutions are compared with measurements in Fig. 9. The characterization of the stub with the doubly-fine 40 $\times$ 40 resolution is carried out according to (22). As shown in Fig. 9, the procedure of

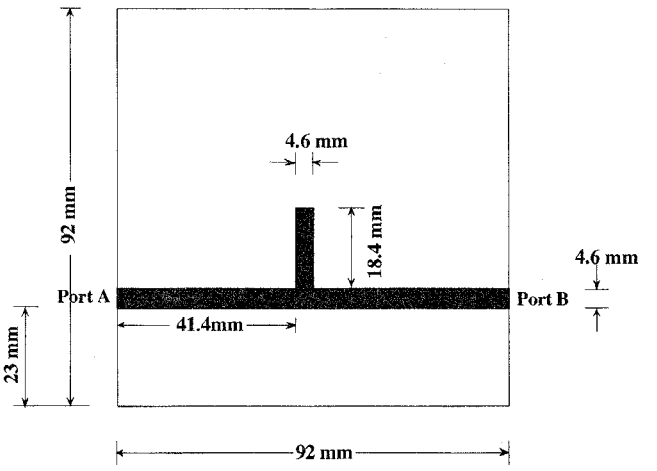


Fig. 7. A shielded microstrip single-stub filter. The shielding rectangular cavity has dimensions 92 mm $\times$ 92 mm $\times$ 11.4 mm, the substrate is RT Duroid 5870 of thickness $t = 1.57$ mm and dielectric constant $\varepsilon_r = 2.33$.

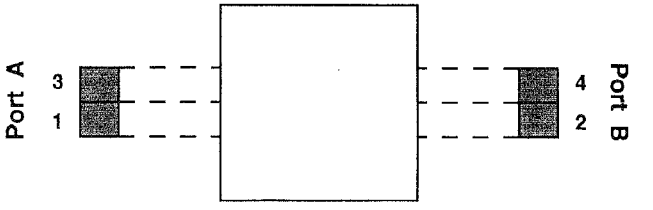


Fig. 8. A schematic for the augmented circuit corresponding to Fig. 7.

Section VII is justified since the 40 $\times$ 40-grid computations indeed recover the results of the 20 $\times$ 20 grid. In calculating these scattering parameters both the delta-gap voltage and the impressed-current models have been implemented and as expected yielded identical results. Furthermore, the computed results are consistent with measurements performed on an HP8510C network analyzer.

## IX. Conclusion

In this work we have dealt with the problem of characterizing microstrip-fed multiport planar passive microwave circuits using the method of moments. For this purpose, we have considered two commonly encountered excitation models: the delta-gap voltage and the impressed-current models. First, we have determined and discussed the fine mathematical and physical conditions under which the two excitation models become equivalent. This was done both from the viewpoint of using the direct definition of the network parameters and when using familiar variational expressions. Based on this equivalence we have shown how to extract network parameters from multiport planar passive circuits in an unambiguous way. This extends to MoM discretization schemes in which some of the ports are transversely multisegmented. Supportive numerical and experimental results for the characterization of shielded planar circuits were also provided.

In our view this is the first time that such a comprehensive treatment of the fine details associated with the subject of characterizing multiport planar circuits using the MoM is being undertaken. Apart from the practical significance of the presented work in characterizing multiport planar circuits,

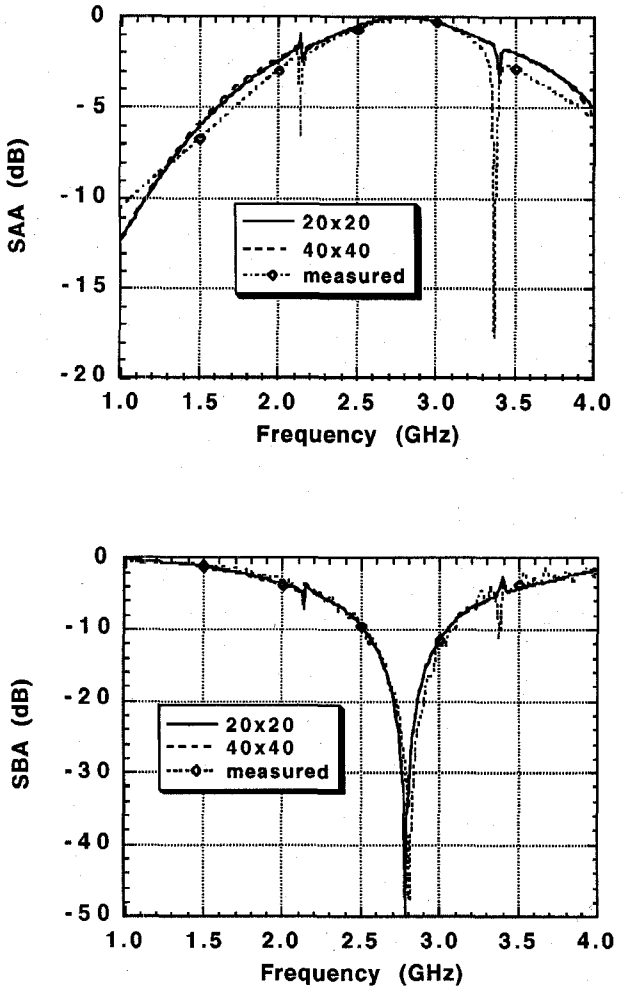


Fig. 9. The computed and measured scattering parameters for the benchmark microstrip filter of Fig. 7, analyzed with 20 × 20 and 40 × 40 grids.

it also serves the purpose of clarifying many aspects of the excitation modeling which undoubtedly still is a constant source of confusion among the MoM community.

## REFERENCES

[1] J. C. Rautio, "A time-harmonic electromagnetic analysis of shielded microstrip circuits," Ph.D. dissertation, Syracuse Univ., Syracuse, NY, 1986.

[2] J. C. Rautio and R. F. Harrington, "An electromagnetic time-harmonic analysis of shielded microstrip circuits," *IEEE Trans. Microwave Theory Tech.*, vol. MTT-35, pp. 726–730, Aug. 1987.

[3] L. P. Dunleavy, "Discontinuity characterization in shielded microstrip: A theoretical and experimental study," Ph.D. dissertation, Univ. of Michigan, Ann Arbor, Apr. 1988.

[4] L. P. Dunleavy and P. B. Katehi, "A generalized method for analyzing thin microstrip discontinuities," *IEEE Trans. Microwave Theory Tech.*, vol. 36, pp. 1758–1766, Dec. 1988.

[5] A. Hill, J. Burke, and K. Kottapalli, "Three-dimensional electromagnetic analysis of shielded microstrip circuits," *Intl. J. Microwave Mm-Wave CAE*, vol. 2, pp. 286–296, 1992.

[6] W. P. Harokopous Jr. and P. B. Katehi, "Electromagnetic coupling and radiation loss considerations in microstrip (M)MIC design," *IEEE Trans. Microwave Theory Tech.*, vol. 39, pp. 413–421, Mar. 1991.

[7] J. R. Mosig, "Arbitrarily shaped microstrip structures and their analysis with a mixed potential integral equation," *IEEE Trans. Microwave Theory Tech.*, vol. 36, pp. 314–323, Feb. 1988.

[8] ——, "Integral equation technique," in *Numerical Techniques for Microwave and Millimeter-Wave Passive Structures*, T. Itoh, Ed. New York: Wiley, 1989, ch. 3.

[9] W. Wertgen and R. H. Jansen, "Efficient direct and iterative electrodynamic analysis of geometrically complex MIC and MMIC structures," *Int. J. Numer. Mod. Electron. Net. Dev. Fields*, vol. 2, pp. 153–164, 1989.

[10] J. C. Rautio, "A de-embedding algorithm for electromagnetics," *Int. J. Microwave and Mm-Wave CAE*, vol. 1, pp. 282–287, 1991.

[11] A. Hill, "Analysis of multiple coupled microstrip discontinuities for microwave and millimeter wave integrated circuits," in *IEEE MTT-S Int. Microwave Symp. Dig.*, 1991, pp. 1091–1094.

[12] A. Skrivervik and J. R. Mosig, "Equivalent circuits of microstrip discontinuities including radiation effects," in *IEEE MTT-S Int. Microwave Symp. Dig.*, 1989, pp. 1147–1150.

[13] T. K. Sarkar, "A note on the choice of weighting functions in the method of moments," *IEEE Trans. Antennas Propagat.*, vol. AP-33, pp. 436–441, Apr. 1985.

[14] G. V. Eleftheriades and J. R. Mosig, "Electromagnetic modeling of passive microwave components, call-off order no 2," Rep. No. LEMA-RT-95-03, Swiss Federal Institute of Technology, Lausanne, Switzerland, Mar. 1995.

[15] G. V. Eleftheriades, M. Guglielmi, and J. R. Mosig, "An efficient mixed potential integral equation technique for the analysis of shielded MMIC's," in *Proc. 25th European Microwave Conf.*, Sept. 1995, pp. 825–829.

[16] R. E. Collin, *Antennas and Radiowave Propagation*. New York: McGraw-Hill, 1985, pp. 465–472.

[17] R. F. Harrington, *Time-Harmonic Electromagnetic Fields*. New York: McGraw-Hill, 1961, ch. 7, pp. 348–355.

**George V. Eleftheriades** (S'85–M'94) was born in Limassol, Cyprus. He received the diploma in electrical engineering with distinction from the National Technical University of Athens, Athens, Greece in 1988, the M.S. and Ph.D. degrees in electrical engineering both from the University of Michigan, Ann Arbor, in 1989 and 1993 respectively.

Currently, he is a Research Associate at the Laboratory of Electromagnetics and Acoustics, Swiss Federal Institute of Technology Lausanne (EPFL), Switzerland. His present research interests include millimeterwave antennas and circuits for wireless applications, planar antennas and circuits for telecommunications, numerical and analytical techniques in electromagnetics, and high-speed digital interconnects.

Dr. Eleftheriades received the Best Paper Award at the 1990 JINA International Conference on Antennas, Nice, France, an IEEE AP-S Student Paper Award in 1993, and the "Distinguished Achievement Award" from the University of Michigan in 1991.

**Juan R. Mosig** (S'76–M'87–SM'94) was born in Cadiz, Spain. He received the electrical engineer degree in 1973 from University Politecnica de Madrid, Spain. In 1975 he joined the Laboratory of Electromagnetics and Acoustics at Ecole Polytechnique Fédérale de Lausanne (EPFL), Switzerland, from which he received the Ph.D. degree in 1983.

Since 1991 he has been an Associate Professor at EPFL. In 1984, he was a Visiting Research Associate at Rochester Institute of Technology, Rochester, NY. He has also held scientific appointments at universities of Rennes (France), Nice (France) and University of Colorado at Boulder. He is the author of four chapters in books on microstrip antennas and circuits. His research interests include electromagnetic theory, numerical methods, and microstrip antennas.